

# Measurement of orthotropic electric conductance of CFRP laminates and analysis of the effect on delamination monitoring with an electric resistance change method

Akira Todoroki\*, Miho Tanaka, Yoshinobu Shimamura

*Department of Mechanical Sciences, and Engineering, Tokyo Institute of Technology, Ohokayama,  
2-12-1, Meguro, Tokyo 152-8552, Japan*

Received 17 July 2001; received in revised form 17 December 2001; accepted 18 December 2001

## Abstract

Since delaminations of composite laminates are usually invisible or difficult to detect by visual inspections, delamination causes low reliability for primary structures. Automatic systems for delamination identifications in-service are desired in order to improve this low reliability. The present study employs an electric resistance change method for detection of delaminations. Since the method adopts reinforcement carbon fibre itself as sensors for delamination detections, this method does not cause reduction of static strength or fatigue strength; also, this method is applicable to existing structures. In the present study, a relationship between fibre volume fraction and orthotropic electric conductivities is confirmed by experimentation and the effect of measured orthotropic electric conductance on delamination monitoring is discussed analytically with FEM analyses. Two types of cross-ply laminates are prepared for delamination monitoring analyses: [0/90]<sub>s</sub> and [90/0]<sub>s</sub>. Electric resistance changes due to delamination creation are discussed for both specimen types with results of electric current density diagrams. As a result, it can be concluded that the fibre volume fraction has a large effect on electric conductance of the transverse and thickness directions, and electric conductance of the thickness direction has significant effects on delamination detection with the electric resistance change method. © 2002 Elsevier Science Ltd. All rights reserved.

*Keywords:* A. Carbon fibre; B. Electrical properties; Electric resistance; C. Delamination

## 1. Introduction

Composite laminates have low delamination resistance; this low resistance induces delaminations by slight out-of-plane impacts. Since delaminations are usually difficult to detect by visually or sometimes invisible, delamination causes low reliability for primary structures. To improve low reliability, automatic systems for delamination identification in-service are desired. A structural integrity monitoring system to detect delaminations is one desired approach for practical laminated composite structures.

Recently, an electric resistance change method was employed to identify internal damage of CFRP (carbon fibre reinforced plastics) laminates by many researchers

[1–18]. The electric resistance change method does not require expensive instruments. Since the method adopts reinforcement carbon fibre itself as sensors for damage detection, this method does not cause reduction of static strength or fatigue strength; also, this method is applicable to existing structures. Moreover, the electric resistance change method does not increase weight.

Authors have already experimentally investigated applicability of the electric resistance change method for delamination crack length measurements of edge cracks in delamination resistance tests [19,20]. For practical composite structures, however, delamination cracks are usually embedded cracks. Embedded cracks of beam type specimens were also experimentally detected with the electric resistance change method by Todoroki using carbon/PEEK composites [21]. To investigate the effect of orthotropic electric resistance on delamination monitoring of cross-ply laminates, several FEM analyses have been also conducted [22,23]. Beam type specimens

\* Corresponding author. Fax: +81-3-5734-3178.

E-mail address: atodorok@ginza.mes.titech.ac.jp (A. Todoroki).

were employed to monitor delamination creation experimentally [24], as were plate type specimens [25]. However, actual orthotropic electric conductance has not been measured and the effect of electric conductance variation has not been investigated in detail. Louis et al. have measured electric resistances of the thickness direction for various laminates [26]. They showed the effect of the stacking sequence on electric resistance in the thickness direction, but did not measure the effect of the fibre volume fraction and did not show the effect of electric resistance change on delamination monitoring.

In the present study, a relationship between fibre volume fraction and orthotropic electric conductance is confirmed experimentally, and the effect of measured orthotropic electric conductance on delamination monitoring is discussed analytically with FEM analyses. Two types of cross-ply laminates were fabricated from three types of carbon fibre volume fraction. The material employed here is Q-111 2500: unidirectional carbon fibre/epoxy prepreg produced by Toho Rayon Co., Ltd. A hot-press method is used for curing, and the curing condition is  $130\text{ }^{\circ}\text{C}\times 50\text{ min}$ . To make specimens of three types of fibre volume fractions, the following processing procedures were performed.

1. The prepreg sheet is cut to rectangular plies of 170 mm length and 80 mm width.
2. The prepreg plies are stacked according to three ply counts: for low volume fraction laminates, the number of plies is 4. For a middle volume fraction laminate, the number of plies is 6. For a high volume fraction laminate, the number of plies is 7.
3. A large sheet of silicone rubber (250 mm $\times$ 250 mm) of 1 mm thickness with a rectangular notch (170 mm $\times$ 80 mm) is placed between the hot-press plates.
4. The stacked laminate is placed inside the rectangular notch of the large silicone rubber sheet.
5. The laminate and silicone rubber sheet are compressed at curing temperature to make a laminate of 1 mm thickness for all three types; these three sheets of various thickness were pressed to produce plates of equal thickness to obtain three different fibre volume fractions. Thickness of all three types of laminates is approximately the same at about 1 mm. By pressing to the same thickness, matrix resin is removed from thicker laminates, producing specimens consisting of three different fibre volume fractions.

After curing, the fibre volume fraction of the three types of laminates was measured by the following process.

1. A small size rectangular specimen is cut from the laminate (see Fig. 1).
2. The side section of the specimen is polished.
3. The number of fibres ( $N$ ) is counted using video images of the small area ( $S$ ) of 1 mm (thickness direction) $\times$ 0.2 mm (width direction).
4. Average diameter ( $d_f$ ) of the fibre is measured at the cross section.
5. Average fibre volume fraction  $V_f$  is calculated from  $V_f = (Nd_f^2\pi/4S)$ .

Electric conductance values of the three directions are measured directly using small specimens. Specimen configurations are shown in Fig. 1(a)–(c), respectively. In order to measure electric resistance of the specimen, silver paste is painted as electrodes. The reason why the video image is used instead of the standard method for volume fraction measurement is to confirm fibre distribution of practical CFRP laminates; the method adopted here is more time consuming.

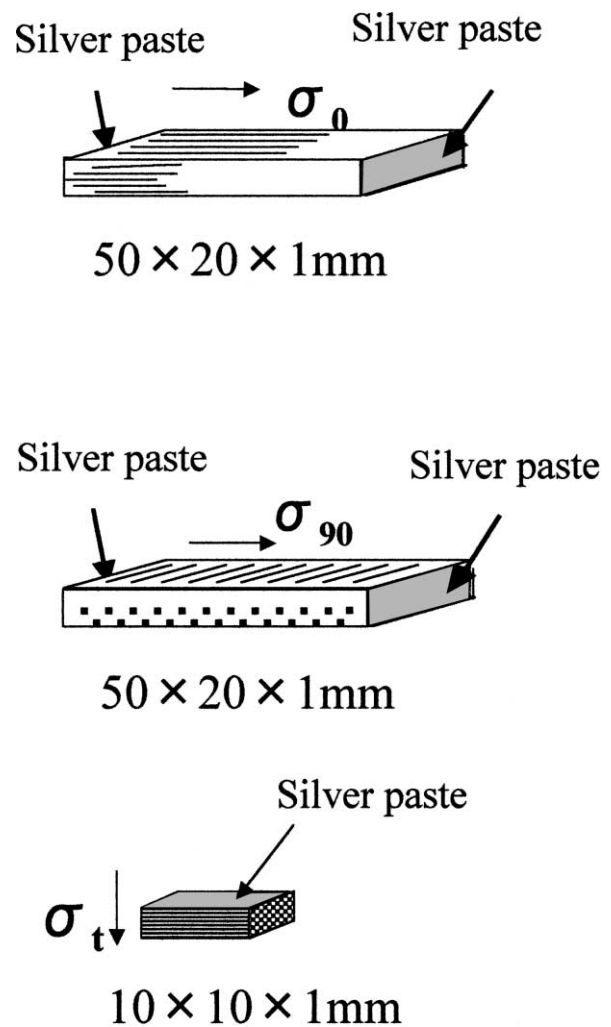


Fig. 1. Specimen configurations for measurements of orthotropic electric conductance.

## 2. Results and discussion

Typical cross section images of the three laminate types are shown in Fig. 2 (a)–(c), respectively. Tens of images for each type of specimen were taken to obtain an entire (composite) cross section image. The total number of carbon fibres was counted, and fibre volume fractions of three types of laminates were measured directly. For the low fibre volume fraction specimen, measured  $V_f$  was 0.40. For the middle fibre volume fraction specimen, measured  $V_f$  was 0.47; and measured  $V_f$  was 0.62 for the high fibre volume fraction specimen. For example, for the case of  $V_f=0.40$ , the number of fibres counted was 2700. These fibre volume fractions are averaged results of ten specimens of each specimen type.

Measured electric conductance of each type of specimen is shown in Table 1. Measured electric conductance values are plotted against fibre volume fractions in Fig. 3 (a)–(c), respectively. In the fibre direction, electric conductance values ( $\sigma_0$ ) of three volume fractions are plotted on a line as shown in the figure. This shows that electric conductance of the fibre direction follows the rule of mixture. The rule of mixture for electric conductance is easily obtained as follows with a parallel-connected spring model.

$$\sigma_0 = \sigma_f V_f + \sigma_m (1 - V_f) \quad 1$$

where  $\sigma_0$  is electric conductance of fibre direction ( $0^\circ$  direction),  $\sigma_f$  is electric conductance of carbon fibre,  $\sigma_m$  is electric conductance of matrix resin and  $V_f$  is the fibre volume fraction. Since the matrix resin is usually an electric insulator,  $\sigma_m$  vanishes. That implies the following relationship.

$$\sigma_0 = \sigma_f V_f \quad 2$$

Eq. (2) represents the linear relationship between electric conductance of fibre direction  $\sigma_0$  and fibre volume fraction  $V_f$ .

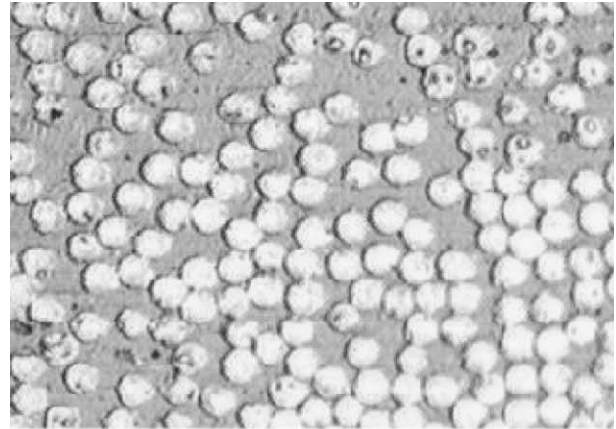
In the transverse direction ( $90^\circ$  direction), electric conductance  $\sigma_{90}$  is calculated from the rule of mixture as follows with a serially connected spring model.

$$\sigma_{90} = \frac{\sigma_f \sigma_m}{\sigma_m V_f + \sigma_f (1 - V_f)} \quad 3$$

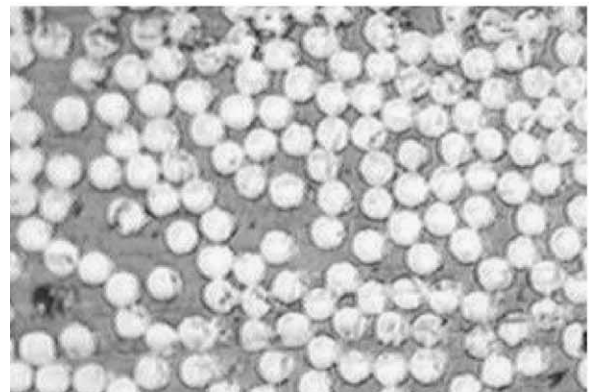
The  $\sigma_{90}$  vanishes from the rule of mixture by substituting  $\sigma_m=0$ . In the same way, electric conductance of the thickness direction  $\sigma_t$  vanishes from the rule of mixture.

Measured values of electric conductance of  $\sigma_{90}$  and  $\sigma_t$  are significantly smaller than  $\sigma_0$ , but they are not zero. Non-zero electric conductance values of non-fibre directions are caused by the carbon fibre network produced

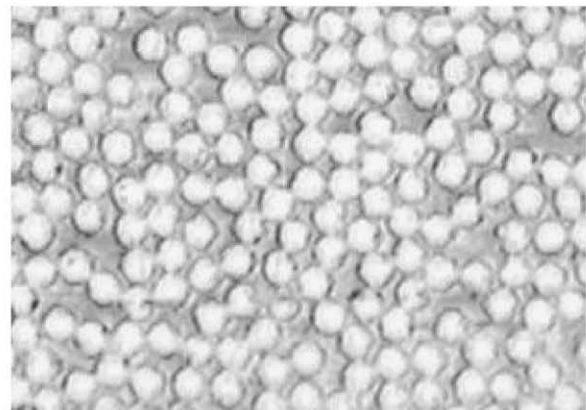
by fibre contacts. Carbon fibre itself is not a straight fibre but a wavy configuration in practical composites as shown in Fig. 4. This wave shape produces many contact points with adjacent fibres. The fibre contact makes



(a)



(b)



(c)

Fig. 2. Specimen cross section of three types of fibre volume fraction.

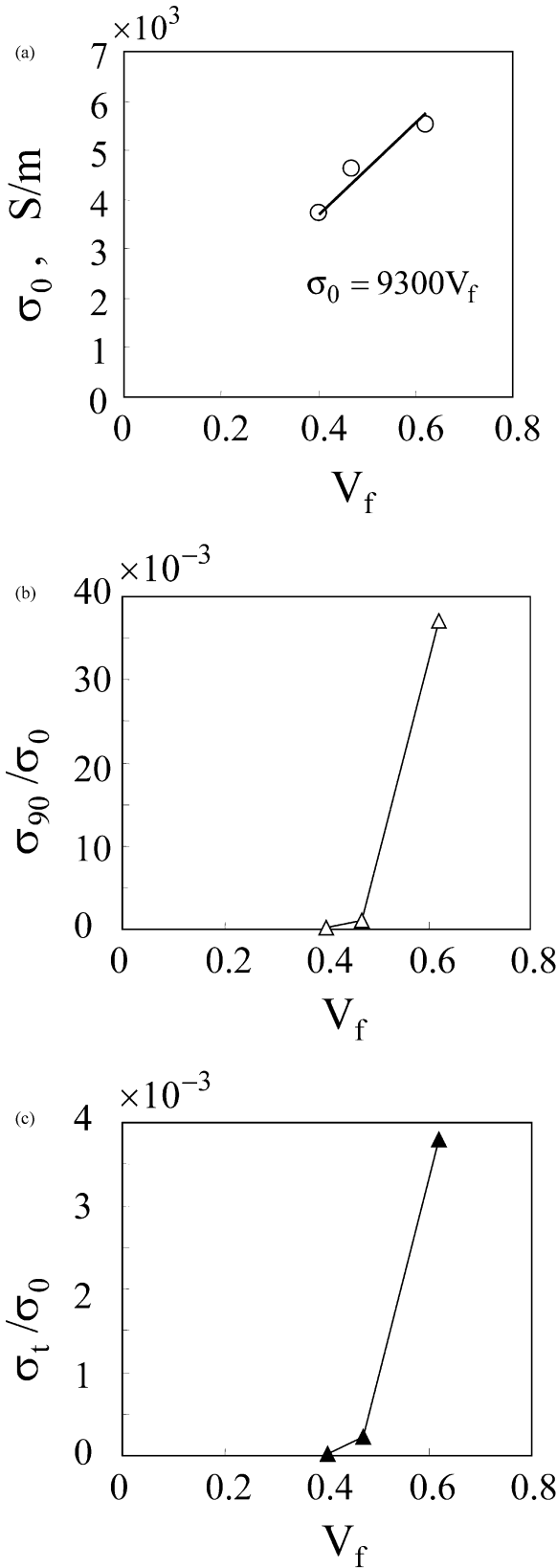


Fig. 3. Measured orthotropic electric conductivity of CFRP laminate. (a) Measured relation between  $V_f$  and electric conductivity of the fibre direction; (b) measured relation between  $V_f$  and electric conductivity ratio of the transverse direction; (c) measured relation between  $V_f$  and electric conductivity ratio of the thickness direction.

transverse electric conductivity of  $\sigma_{90}$ . Similar characteristics are notable for electric conductivity of the thickness direction. However, resin rich interlamina exist in the thickness direction. The interlamina make the electric conductivity of  $\sigma_t$  smaller than  $\sigma_{90}$ . Since electric conductivity of  $\sigma_{90}$  and  $\sigma_t$  depends on fibre contacts due to random wavy configuration of the fibre, these small electric conductivity values of  $\sigma_{90}$  and  $\sigma_t$  vary significantly by the slight change of fibre volume fraction as shown in Fig. 3.

### 3. Effect of orthotropic electric conductivity

#### 3.1. Computational method and model

In this study, FEM analyses are employed for investigations of the effect of orthotropic electric conductivity values on delamination monitoring. Beam type specimens were adopted for FEM analyses of delamination monitoring as shown in Fig. 5. Beam length is 140 mm and beam thickness is 2 mm. Two types of stacking sequences are computed here: [0/90]s

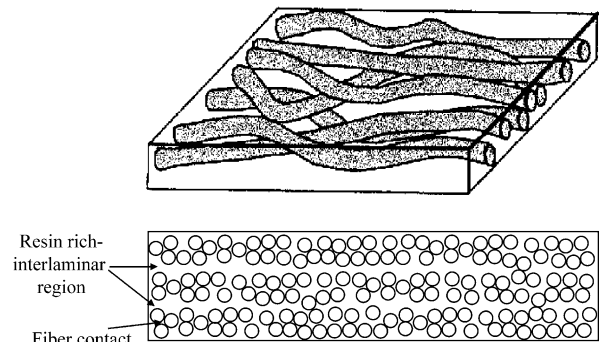


Fig. 4. Schematic model of actual carbon fibre network due to fibre contacts.

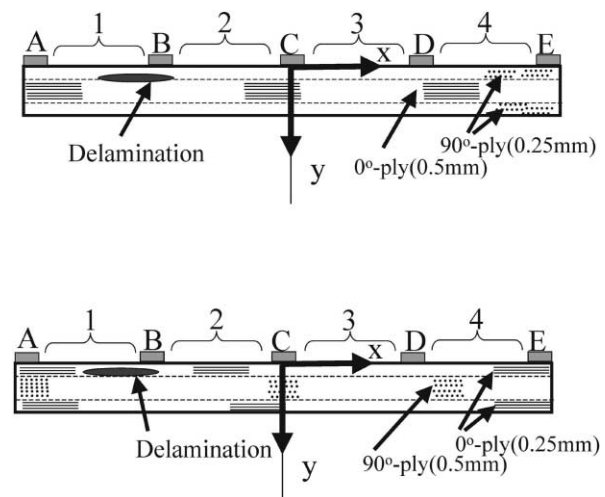


Fig. 5. Specimen configuration for delamination monitoring. (a) Laminate of [0/90]s; (b) laminate of [90/0]s.

and [90/0]s. In this study, ply thickness is fixed at 0.5 mm, four times larger than the normal prepreg.

The authors have performed delamination monitoring for identification of delamination size and location using the electric resistance change method [19–25]. In this method, multiple electrodes are mounted on the laminate surface and electric resistance change after creation of a delamination is measured in each segment between electrodes. For example, let us consider the case of a five-electrode-beam specimen. In this case, five electrodes are mounted on the specimen top surface. The specimen consequently has four segments between electrodes, and electric resistance changes of the four segments are measured after creation of a delamination. A large number of data sets of electric resistance changes are collected and these sets of data are used for showing a relationship between measured electric resistance changes and the delamination crack. Since it is an inverse problem to obtain delamination location and size from the measured set of electric resistance changes, authors have adopted artificial neural networks and response surfaces to obtain the relationship [27]. Using this relationship, delamination location and size (length) can be successfully monitored [24,25,27]. The reason why all electrodes are mounted on the specimen top is to simulate internal monitoring of thin shell type structures such as aerospace structures.

Since carbon fibre diameter is much smaller than the size of FEM elements adopted here, the inhomogeneous

orthotropic CFRP composite material is assumed to be homogeneous orthotropic material for present FEM analysis. In the thickness direction, however, the thickness of the resin rich layer, which causes lower electric conductance compared to that of the transverse direction, is not less than the ply thickness. This introduces the difficulty of modeling electric conductance in the thickness direction. In the present study, four-node-rectangular elements are adopted for analysis; each element is approximately  $0.125 \text{ mm} \times 0.125 \text{ mm}$ . Since ply thickness is 0.5 mm, a ply comprises four elements in the thickness direction. This implies that average electric conductance in the thickness direction in a ply can be obtained by assuming homogeneous electric conductance in the thickness direction. Electric conductance in the thickness direction, therefore, is treated as approximately homogeneous here.

FEM analyses are performed using a commercially available FEM tool named ANSYS. By using the ANSYS auto mesh generation system the specimen model is divided into 2-dimensional elements numbering approximately 19,200. On delamination crack surface lines, all nodes are doubly defined to represent delamination crack surfaces. When a delamination crack is created, doubly defined nodes on delamination crack surfaces are released with each other to represent electric current insulation. In the present study, therefore, for a delamination crack induced in the FEM model, it is assumed that the crack mouth is fully opened after delamination.

Electric conductance data used for FEM analysis are the three sets of measured orthotropic electric conductance shown in Table 1. In order to compute electric resistance change, direct electric current of 30 mA is charged from the electrode of A and electric voltage of electrode B is set to 0 V. After computation, electric voltage at electrode A is obtained and the electric voltage value is divided by electric current (30 mA) to calculate electric resistance of the segment between electrodes A and B.

Table 1

$V_f$	$\sigma_0$ (S/m)	$\sigma_{90}/\sigma_0$	$\sigma_t/\sigma_0$
0.40	3700	$1.8 \times 10^{-4}$	$1.6 \times 10^{-5}$
0.47	4600	$1.1 \times 10^{-3}$	$2.2 \times 10^{-4}$
0.62	5500	$3.7 \times 10^{-2}$	$3.8 \times 10^{-3}$

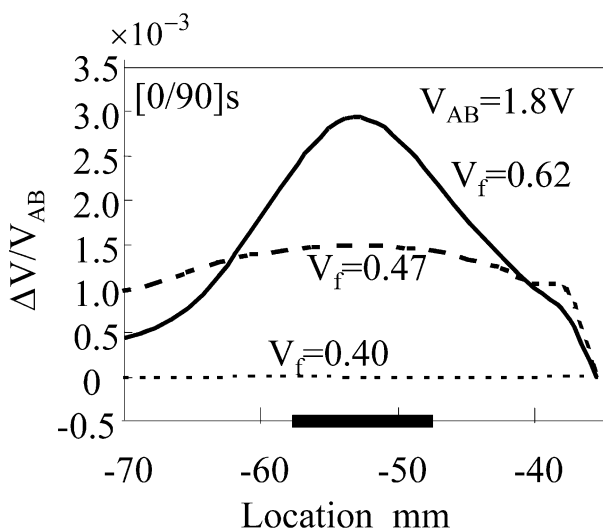


Fig. 6. Electric voltage change distribution due to [0/90]s delamination.

### 3.2. Computational results and discussion

Electric voltage distribution results of three cases of the fibre volume fractions for the laminate of [0/90]s are shown in Fig. 6 (electric current is charged in the fibre direction of the surface ply). The abscissa is the location between electrode A ( $-70 \text{ mm}$ ) and B ( $-35 \text{ mm}$ ). The ordinate is electric voltage change ( $\Delta V$ ) due to delamination divided by initial electric voltage between electrodes A and B ( $V_{AB} = 1.8 \text{ V}$ ). Delamination is located between  $x = -57.5 \text{ mm}$  and  $x = -47.5 \text{ mm}$  at the inter-lamina between the upper  $0^\circ$  ply and the middle  $90^\circ$  ply (size is 10 mm). Since electrode B ( $x = -35 \text{ mm}$ ) is fixed at 0 V, the electric resistance change ratio between A and B ( $\Delta R/R_{AB}$ ) can be obtained as follows.

$$\frac{\Delta R}{R_{AB}} = \frac{\Delta V}{V_{AB}}$$

$$= \frac{(V_{\text{after delamination}} - V_{\text{before delamination}})_{x=-70}}{V_{x=-70, \text{ before delamination}}} \quad 4$$

In the case of  $V_f=0.40$  (the strongest orthotropic case), no electric resistance change is observed as shown with the dotted line in the figure. Even just over the delamination crack (from  $-47.5$  to  $-57.5$  mm), no electric voltage change is observed. In the case of  $V_f=0.47$  (the middle orthotropic case) and  $V_f=0.62$  (the lowest orthotropic case), electric resistance changes between the electrodes are observed. This means that the delamination crack can be detected by the electric resistance change of the segments between the electrodes in both cases.

The electric resistance change ratio of  $V_f=0.47$  (broken curve) is, however, higher than that of  $V_f=0.62$

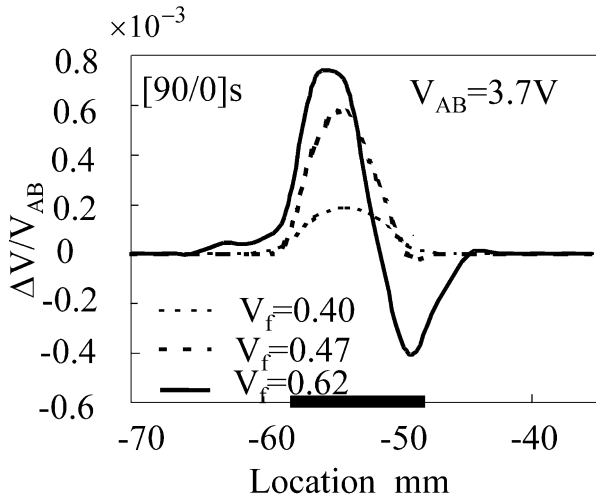


Fig. 7. Electric voltage change distribution due to [90/0]s delamination.

(solid curve). This implies that higher fibre volume fraction (lower orthotropic conductance) is not better for the detection of delamination crack with the electric resistance change method.

On the other hand, electric voltage change at the location over the delamination crack (from  $-47.5$  to  $-57.5$  mm) of  $V_f=0.62$  is higher than that of the case of  $V_f=0.47$ . The smaller difference of electric conductance of the thickness direction becomes, the higher the electric voltage change over the delamination crack location becomes.

Similar electric voltage change is observed also for the laminate of [90/0]s. Electric voltage changes are shown in Fig. 7. For the laminate of [90/0]s, electric conductance of the ratio between the thickness direction and the longitudinal direction (transverse direction) is only 1/10, and this means that orthotropy of the electric conductance of the laminate of [90/0]s is smaller than the case of  $V_f=0.62$  of the laminate of [0/90]s. For all these cases (electric current is charged in the transverse direction of the surface ply), no electric resistance change is observed between electrodes A and B. Large electric voltage changes are, however, observed at the location of the delamination crack the same as that of the case of  $V_f=0.62$  of the laminate of [0/90]s. The smaller the difference of electric conductance, the larger the electric voltage change at the delamination crack location becomes. Note that the delamination crack cannot be detected with the electric resistance change method when electric current is charged in the transverse direction of the surface ply.

Electric voltage contour plots inside specimens of each laminate without a delamination crack are shown in Figs. 8 and 9. For comparison, an electric voltage contour plot of the completely isotropic material is shown in Fig. 10. For the [0/90]s laminate, the hill of the voltage contour around electrode A ( $-70$  mm) descends in a gradual slope even in the thickness direction as

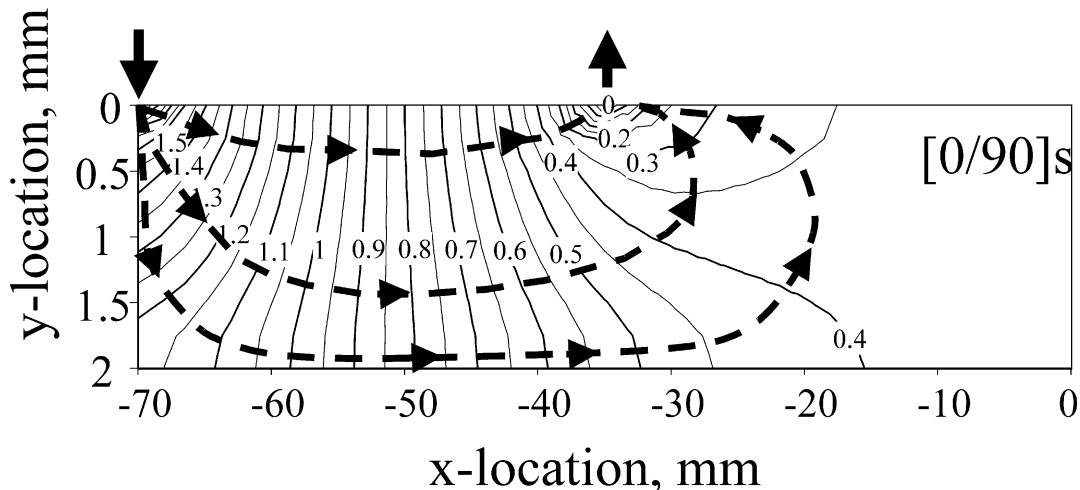


Fig. 8. Contour plot of electric voltage for the [0/90]s laminate.

shown in Fig. 8. This gradual slope creates gradual electric current in the thickness direction; the current indicates an electric resistance change if a delamination crack exists. On the other hand, for the [90/0]s laminate, the slope is very steep and the electric current direction is horizontal between the segment (from -70 to -35 mm) similar to that of the isotropic material (Fig. 10). This causes no electric resistance change between electrodes for the [90/0]s laminate even if a delamination crack exists.

The most noticeable aspect is circular electric current shown in Fig. 8 outside of the charged segment (the region of  $x > -35$  mm). Distribution of electric current density of longitudinal direction ( $x$ -direction) for the [0/90]s laminate is shown in Fig. 11. The abscissa is electric current density of the  $x$ -direction ( $D_x$ ) and the ordinate is location of the thickness direction at the cross section of the delamination crack. For the [0/90]s laminate, most electric current flows in both of the 0° plies (surface and bottom plies). Electric current density of the bottom 0° ply is produced by electric current flow in the thickness direction. Distribution of electric current of

the thickness direction ( $y$ -direction) for the [0/90]s laminate is shown in Fig. 12. The abscissa is the location of  $x$ -direction and the ordinate is electric current density of the  $y$ -direction ( $D_y$ ) at the cross section of  $y=0.5$  (between the top 0° ply and the middle 90° ply). As shown in this figure, electric current of the  $y$ -direction exists around both electrodes. Positive electric current density of the  $y$ -direction indicates downward electric current, and the negative one means upward current. Downward electric current exists near the plus electrode A (-70 mm) and upward electric current exists near the minus electrode B (-35 mm). Due to downward electric current, electric current in the bottom 0° ply is produced. Since electric current of the bottom 0° ply does not return to the top 0° ply immediately at electrode B due to greatly different electric conductance, the electric current returns to the top 0° ply even outside of the segment between A and B from the bottom 0° ply.

Electric current density of  $x$ -direction at the cross section outside of the segment is shown in Fig. 13. The abscissa is electric current density of  $x$ -direction ( $D_x$ ) and the ordinate is location of thickness direction.

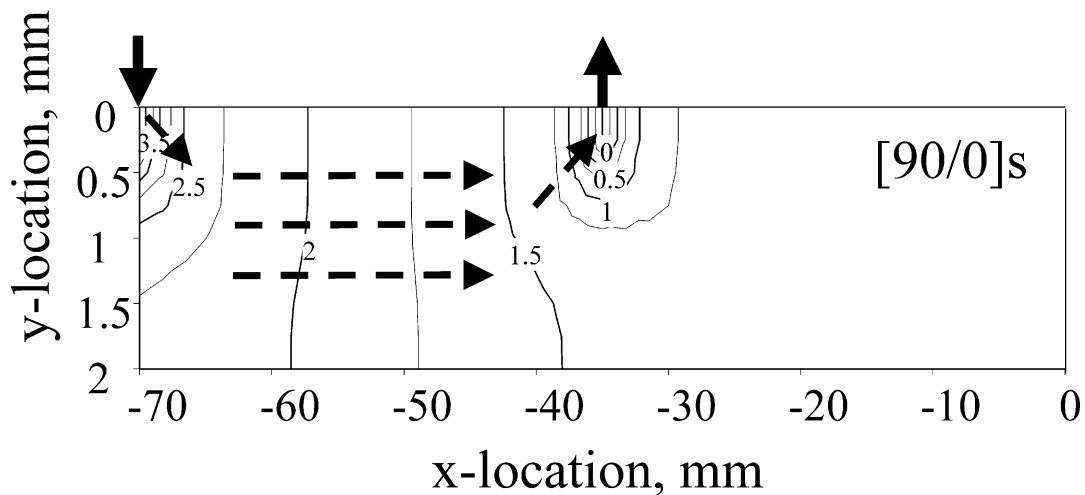


Fig. 9. Contour plot of electric voltage for the [90/0]s laminate.

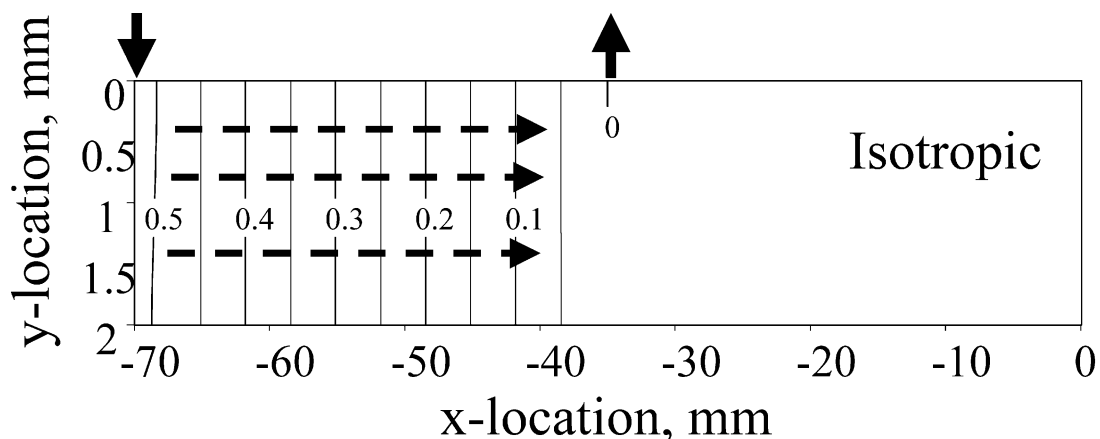


Fig. 10. Contour plot of electric voltage for an isotropic plate.

Negative electric current density exists in the top 0° ply, and positive electric current exists in the bottom 0° ply as shown in this figure. This implies that circular electric current exists outside of the charged segment.

Electric current of the y-direction outside of the charged segment introduces another difficulty. This circular electric current causes electric resistance change due to delamination existing outside of the charged segment. Fig. 14 shows results of electric resistance changes in all segments when delamination exists at the number 2 segment. The abscissa is the segment number and the ordinate is electric resistance changes calculated

at each segment. For example, electric resistance change at the number 3 segment means that electric resistance change between electrodes C and D when an electric current of 30 mA is charged at electrode C and electric voltage at electrode D is set to 0 V. Note that a delamination exists outside of segment number 3 (delamination exists in segment number 2) in this case. Highest electric resistance change is observed at segment number 1, which is a different segment from the segment where the delamination crack exists. This phenomenon agrees with experimental results of CFRP beams in our previous study [24]. This requires a complicated tool for

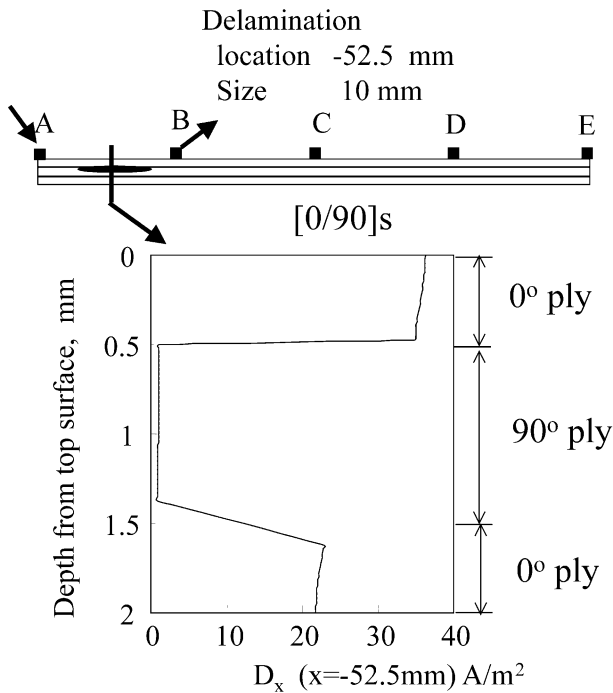


Fig. 11. Electric current density of the longitudinal direction ( $D_x$ ) at the cross section between charged electrodes A and B.

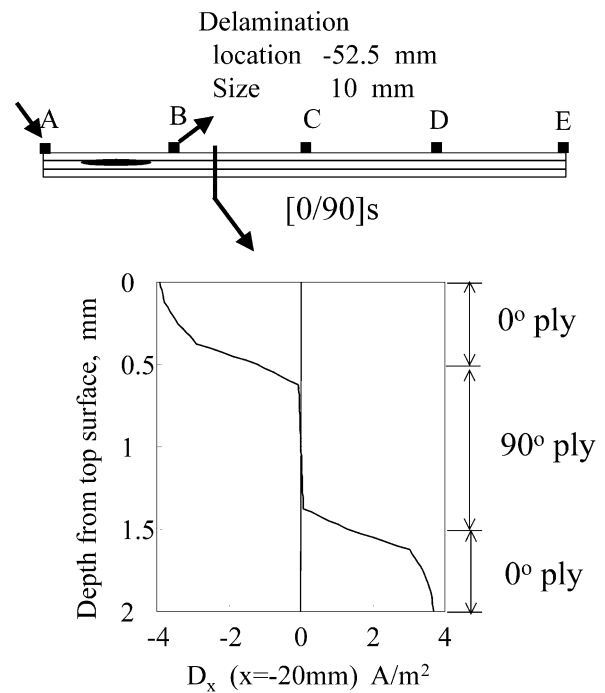


Fig. 13. Electric current density of the longitudinal direction ( $D_x$ ) at the cross section outside of the charged electrodes.

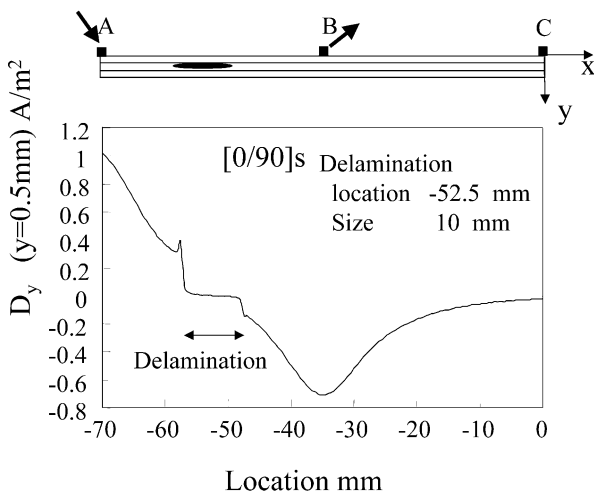


Fig. 12. Electric current density of the thickness direction ( $D_y$ ) at the cross section of  $y=0.5$  mm.

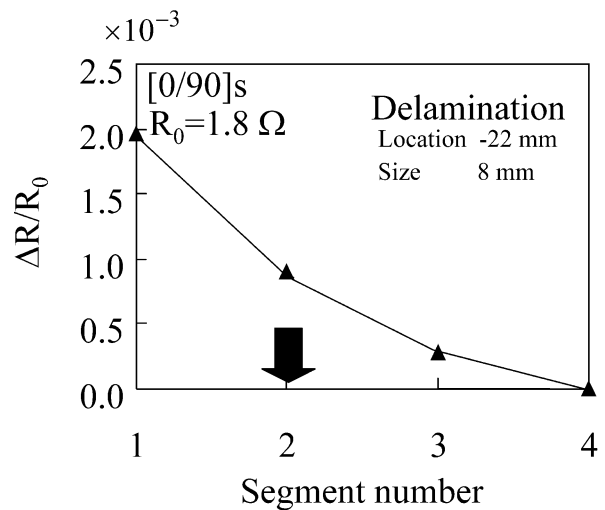


Fig. 14. Electric resistance change distribution when delamination exists at segment number 2.

solving the inverse problem to predict delamination location and size from measured electric resistance changes of electrode segments. As previously mentioned, this problem has been solved with artificial neural networks and response surface method in our previous study [27].

#### 4. Conclusions

This study measured the effect of fibre volume fraction on electric conductance of CFRP laminates and analyzed, with FEM analysis, the effect of orthotropic electric conductance on detection of a delamination crack with electric resistance change between electrodes. Results obtained are as follows.

1. Electric conductance of the fibre direction of a CFRP laminate can be obtained from the volume fraction of carbon fibre and carbon fibre conductance. On the other hand, electric conductances in the transverse direction and thickness direction are not zero and are significantly affected by the fibre volume fraction. Electric conductance of the thickness direction is one tenth the electric conductance of the transverse direction due to resin rich layers.
2. Due to greatly different electric conductance in the thickness direction, electric current flows gradually in the thickness direction, enabling delamination crack detection with electric resistance change between electrodes when the electric current is charged in the fibre direction. When the electric current is charged in the transverse direction, delamination cracks cannot be detected with electric resistance change between electrodes.
3. Due to largely different electric conductance in the thickness direction, the circular electric current is induced outside of the charged segment between electrodes. This current brings electric resistance change in segments adjacent to a segment with a delamination crack.

#### References

- [1] Moriya K, Endo T A. Study on flaw detection method for CFRP composite laminates (1st report) the measurement of crack extension in CFRP composites by electrical potential method. *Aeronautical and Space Science Japan*, 1988;36(410):139–146 [in Japanese].
- [2] Schulte K, Baron C. Load and failure analyses of CFRP laminates by means of electrical resistivity measurements. *Composite Science and Technology* 1989;36:63–76.
- [3] Muto N, Yanagida H, Miyayama M, Nakatsuji T, Sugita M, Ohtsuka Y. Foreseeing of fracture in CFGFRP composites by measuring electric resistance. *Journal of the Japan Society for Composite Materials*, 1992;18(4):144–150 [in Japanese].
- [4] Fischer Chr, Arendts FJ. Electrical crack length measurement and the temperature dependence of the mode I fracture toughness of carbon fibre reinforced plastics. *Composite Science and Technology* 1993;46:319–23.
- [5] Chen PW, Chung DDL. Carbon fibre reinforced concrete for smart structures capable of non-destructive flaw detection. *Struct Smart Mater* 1993;2:22–30.
- [6] Kaddour AS, Al-Salehi FA, Al-Hassani STS. Electrical resistance measurement technique for detecting failure in CFRP materials at high strain rate. *Composite Science and Technology* 1994;51:377–85.
- [7] Wolfger C, Drechsler K. Damage detection in composite materials by monitoring electrical impedance. In: *Proc. of the Int. Symp. on Advanced Materials for Lightweight Structures*, ESTEC, Noordwijk (ESA-WPP-070) 1994 pp. 677–782.
- [8] Chen PW, Chung DDL. Carbon-fibre-reinforced concrete as intrinsically smart concrete for damage assessment during dynamic loading. *J Am Ceram Soc* 1995;78(3):816–8.
- [9] Wang X, Chung DDL. Sensing delamination in a carbon fibre polymer-matrix composite during fatigue by electrical resistance measurement. *Polymer Composites* 1997;18(6):692–700.
- [10] Irving PE, Thiagarajan C. Fatigue damage characterization in carbon fibre composite materials using an electric potential technique. *Smart Materials and Structures* 1998;7:456–66.
- [11] Abry JC, Bochart S, Chateauminois A, Salvia M, Giraud G. In situ detection of damage in CFRP laminates by electric resistance measurements. *Composite Science and Technology* 1999;59:925–35.
- [12] Seo DC, Lee JJ. Damage detection of CFRP laminates using electrical resistance measurement and neural network. *Composite Structures* 1999;47:525–30.
- [13] Abry JC, Choi YK, Chateauminois A, Dalloz B, Giraud G. In-situ monitoring of damage in CFRP laminates by means of AC and DC measurements. *Composite Science and Technology* 2001;61:855–64.
- [14] Weber I, Schwartz P. Monitoring bending fatigue in carbon-fibre/epoxy composite strands: a comparison between mechanical and resistance techniques. *Composite Science and Technology* 2001;61:849–53.
- [15] Muto N, Arai Y, Shin SG, Matsubara H, Yanagida H, Sugita M, Nakatsuji T. Hybrid composites with self-diagnosing function for preventing fatal fracture. *Composite Science and Technology* 2001;61:875–83.
- [16] Kupke M, Schulte K, Schuler R. Non-destructive testing of FRP by DC and AC electrical method. *Composite Science and Technology* 2001;61:837–47.
- [17] Schueler R, Joshi SP, Schulte K. Damage detection in CFRP by electrical conductance mapping. *Composite Science and Technology* 2001;61:921–30.
- [18] Kubo S, Kuchinishi M, Sakagami T, Ioka S. Identification of delamination in layered composite materials by the electric potential CT method, applied electromagnetics and mechanics, In: Takagi T, Uesaka M. editors *Proc. of the 10th Int. Symp. on Applied Electromagnetics and Mechanics*, Japan Soc. Applied Electromagnetics and Mechanics. 2001 p. 641–2.
- [19] Todoroki A, Matsuura K, Kobayashi H. Application of electric potential method to smart composite structures for detecting delamination. *JSME International J, Series A* 1995;38(4):524–30.
- [20] Todoroki A, Kobayashi H, Matsuura K. Application of electrical potential method as delamination sensor for smart structures of graphite/epoxy. In: Inoue K, Shen SIY, Taya M, editors. *US-Japan Workshop on Smart Materials and Structures*. University of Washington: TMS, 1997. p. 47–54.
- [21] Todoroki A. Delamination detection by electric resistance change for graphite/PEEK composites. *Proceedings of the 5th Japan International S.A.M. PE Symposium* 1997:899–904.
- [22] Todoroki A, Suzuki H, Kobayashi H, Nakamura H, Shimamura Y. Evaluation of orthotropic electrical resistance for delamina-

- tion detection of CFRP by electrical potential method. Transactions of the Japan Society of Mechanical Engineers Series A 1998;64(622):1654–16593 [In Japanese].
- [23] Todoroki A, Suzuki H. Health monitoring of internal delamination cracks for graphite/epoxy composites by electric potential method. *Applied Mechanics and Engineering* 2000;5(1): 283–94.
- [24] Todoroki A, Tanaka Y, Shimamura Y. Response surface for delamination monitoring of graphite/epoxy composite using electric resistance change. In: Chang FK, editor. *Structural Health Monitoring 2000*. Technomic, 1999. p. 308–16.
- [25] Todoroki A., Tanaka Y., Shimamura Y. Electric resistance change method for identification of embedded delamination of CFRP plates materials science research international. *Special Technical Publication-2, JSMS*. 2001. p. 139–45.
- [26] Louis M, Joshi SP, Brockmann W. An experimental investigation of through-thickness electrical receptivity of CFRP laminates. *Composites Science and Technology* 2001;61:911–9.
- [27] Todoroki A. Effect of number of electrodes and diagnostic tool for delamination monitoring of graphite/epoxy laminates using electric resistance change. *Composite Science and Technology* 2001;61(13):1871–80.